



Transition metal complexes bearing atropisomeric saturated NHC ligands

Mariia Savchuk, Lucas Bocquin, Muriel Albalat, Marion Jean, Nicolas Vanthuyne, Paola Nava, Stéphane Humbel, Damien Hérault, Hervé Clavier

► To cite this version:

Mariia Savchuk, Lucas Bocquin, Muriel Albalat, Marion Jean, Nicolas Vanthuyne, et al.. Transition metal complexes bearing atropisomeric saturated NHC ligands. *Chirality*, 2022, 34 (1), pp.13-26. 10.1002/chir.23378 . hal-03500191

HAL Id: hal-03500191








<https://hal.science/hal-03500191>

Submitted on 21 Dec 2021

HAL is a multi-disciplinary open access archive for the deposit and dissemination of scientific research documents, whether they are published or not. The documents may come from teaching and research institutions in France or abroad, or from public or private research centers.

L'archive ouverte pluridisciplinaire **HAL**, est destinée au dépôt et à la diffusion de documents scientifiques de niveau recherche, publiés ou non, émanant des établissements d'enseignement et de recherche français ou étrangers, des laboratoires publics ou privés.

Transition metal complexes bearing atropisomeric saturated NHC ligands

Mariia Savchuk | Lucas Bocquin | Muriel Albalat  | Marion Jean  |
Nicolas Vanthuyne  | Paola Nava  | Stéphane Humbel  |
Damien Hérault  | Hervé Clavier 

Aix Marseille Univ, CNRS, Centrale
Marseille, iSm2, Marseille, France

Correspondence

Hervé Clavier, CNRS, Centrale Marseille,
iSm2, Aix Marseille Univ, Marseille,
France.
Email: herve.clavier@univ-amu.fr

Funding information

Agence Nationale de la Recherche, Grant/
Award Number: ANR-20-CE07-0030

Abstract

From achiral imidazolinium salts, chiral transition metal complexes containing an N-heterocyclic carbene (NHC) ligand were prepared (metal = palladium, copper, silver, gold, rhodium). Axial chirality in these complexes results from the formation of the metal-carbene bond leading to the restriction of rotation of dissymmetric *N*-aryl substituents about the C–N bond. When these complexes exhibited a sufficient configurational stability, a resolution by chiral high-performance liquid chromatography (HPLC) on preparative scale enabled isolation of enantiomers with excellent enantiopurities (>99% ee) and good yields. A study of the enantiomerization barriers revealed the effect of the backbone nature as well as the type of transition metal on its values. Nevertheless, the evaluation of palladium-based complexes in asymmetric intramolecular α -arylation of amides demonstrated that the ability to induce an enantioselectivity cannot be correlated to the configurational stability of the precatalysts.

KEYWORDS

axial chirality, copper, cross coupling reactions, gold, N-heterocyclic carbene ligands, palladium, rhodium, silver

1 | INTRODUCTION

The use of N-heterocyclic carbenes (NHC) as ancillary ligands in various metal complexes has substantially contributed to the development of transition metal catalysis with major achievements for instance in ruthenium-catalyzed olefin metathesis or palladium-catalyzed cross coupling reactions.^{1–3} Therefore, the design and the synthesis of chiral NHC ligands have attracted much attention during the last two decades.^{4–6} The main strategies that have been investigated to design chiral monodentate NHC ligands can be

divided into two categories: the introduction of a chiral element on the *N*-substituents (Figure 1A, structures **A** and **B**) or the use of a chiral NHC backbone (structures **C** and **D**). Most of these chiral NHCs have been synthesized from building blocks coming from the chiral pool and containing stereogenic centers. The implementation of planar chirality to the design of chiral NHC ligands has been scarcely investigated.^{7–11} By comparison, NHC ligands containing axes of chirality have received slightly more attention.^{11–21} The large majority of these ligands contain a binaphthyl moiety, and the complexes bearing such NHCs were found to be efficient in various reactions such as ruthenium-catalyzed metathesis and gold-catalyzed transformations. Recently, we have disclosed a new design of metal–NHC complexes containing an axis of chirality.^{22,23} As depicted in Figure 1C, the concept is

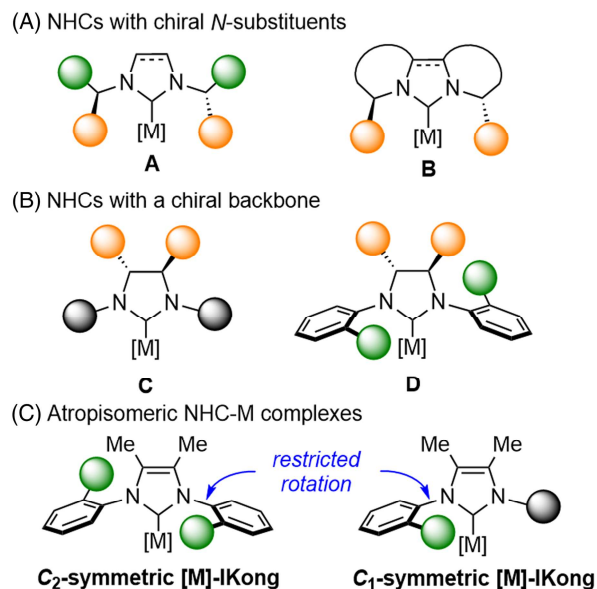


FIGURE 1 Design of chiral NHC-metal complexes

based on a restricted rotation of dissymmetric *N*-aryl substituents about the C–N axis. The advantage of this concept is that synthons arising from the chiral pool are not required for the synthesis of imidazolium salts, precursors of NHC, because the metalation step enables the formation of atropisomers. Owing to the good stability of NHC-metal complexes towards purification by silica gel chromatography, enantiomers resolutions could be achieved using chiral high-performance liquid chromatography (HPLC) in preparative scale (up to 600-mg scale).²² *C*₂-symmetric Pd- and Cu-IKong complexes exhibited good performances in asymmetric catalysis with chiral inductions exceeding 90% ee. Even if *C*₁-symmetric Cu-IKong complexes gave good results in copper-catalyzed asymmetric allylic alkylation, these dissymmetric NHC ligands are interesting to accurately investigate their configurational stability, in particular the values of rotational barriers of the NHC-metal complexes. With NHC-Pd complexes, it has been demonstrated that an unsaturated backbone substituted with methyl groups was required to obtain configurationally stable complexes **3** (Figure 2). With an unsubstituted backbone, unsaturated (complexes **1**) or saturated (complexes **2**), enantiomers could not be observed by chPLC analyses suggesting low rotational barriers values.²³ This statement was confirmed by theoretical calculations, which allowed to quantify enantiomerization barriers with a reasonable level of confidence in addition to predict on which side the most favorable rotation will take place.

Therein, we disclosed the synthesis of dissymmetric imidazolium salts possessing a *gem*-dimethyl moiety and their use to prepare metal–NHC complexes such as palladium complex **4**. The resolution of these axial chirality-containing complexes by chiral HPLC as well as

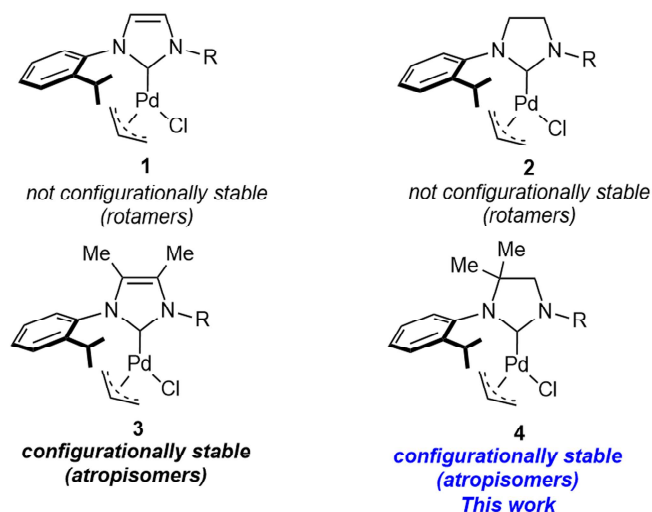


FIGURE 2 Key role of the backbone substitution to restrict rotations about the C–N axis

their configurational stabilities (determination of the rotational barriers values) were investigated.

2 | MATERIALS AND METHODS

All reagents were obtained from commercial sources and used as received. Solvents (THF, DCM, toluene and Et₂O) were purified and dried over Braun solvent purification system (MB-SPS-800) or dried by standard procedures prior to use.²⁴ Analytical Thin Layer Chromatography (TLC) was carried out on Merck silica gel60 F₂₅₄. Products were revealed by ultraviolet light (254 or 366 nm) and stained with dyeing reagents solutions as potassium permanganate solution or *p*-anisaldehyde solution in ethanol followed by gentle heating. Flash chromatography was performed on Combiflash[®] Companion or with Merck silica gel 60 (230–400 mesh). ¹H, ¹³C and ¹⁹F spectra were recorded in CDCl₃ at ambient temperature on Bruker Avance III 300 or 400 spectrometers operating at 300, 400 and 500 MHz respectively for ¹H. ¹³C nuclei was observed with ¹H decoupling. Solvent residual signals were used as internal standard.²⁵ Chemical shifts (δ) and coupling constants (*J*) are given in ppm and Hz, respectively. The peaks patterns are indicated as the following format multiplicity (s: singlet; d: doublet; t: triplet; q: quartet; sept: septuplet; m: multiplet; dd: doublet of doublet; dt: doublet of triplet; dm: doublet of multiplet, etc.). The prefix br. indicates a broadened signal and p. for a pseudo multiplicity. Melting points (uncorrected) were determined with a Büchi Melting Point B-545. IR spectra were obtained using a Bruker Alpha Platinum ATR. HRMS were recorded on SYNAPT G2 HDMS (Waters) or on QStar Elite (Applied Biosystems SGIEX) equipped with an Atmospheric Pressure

Ionization (API) source. Mass spectra were obtained using a time-of-flight (TOF) analyzer. Preparative chiral HPLC separations were performed on an Agilent 1260 Infinity unit (pump G1311C, autosampler G1329B, DAD G1365D, and fraction collector G1364C), monitored by Agilent OpenLAB CDS Chemstation LC. Optical rotations were measured on a Jasco P-2000 polarimeter with a sodium lamp (589 nm), a halogen lamp (578, 546, 436, 405, 365, and 325 nm), in a 10-cm cell, thermostated at 25°C with a Peltier controlled cell holder. Electronic circular dichroism (ECD) and UV spectra were measured on a JASCO J-815 spectrometer equipped with a JASCO Peltier cell holder PTC-423 to maintain the temperature at 25.0 ± 0.2°C. A CD quartz cell of 1 mm of optical path length was used. The CD spectrometer was purged with nitrogen before recording each spectrum, which was baseline subtracted. The baseline was always measured for the same solvent and in the same cell as the samples. Acquisition parameters: 0.1 nm as intervals, scanning speed 50 nm/min, band width 2 nm, and 3 accumulations per sample. The spectra are presented without smoothing and further data processing. X-ray Diffraction: Intensity data were collected on an Agilent SuperNova AtlasS2 diffractometer using MoK α radiation (0.71073 Å) at 293(2) K or D8 VENTURE Bruker AXS diffractometer equipped with a (CMOS) PHOTON 100 detector using MoK α radiation (0.71073 Å) at T = 150 K. Data reduction was performed using the CrysAlisPro software package (version 1.171.37.31) or SHELXT program. The structures were resolved using the software SHELXS-97 by the direct methods and refined using SHELXL-2013-4. The CIF files of transition metal complexes have been deposited with CCDC numbers 2094763 (**5a**), 2094764 (**6a**) and 2094765 (**(R_a)-(–)-7a**).

2.1 | General procedure for the synthesis of the NHC-palladium complexes **4a** and **4c**

A mixture of imidazolium tetrafluoroborate **12** (2.3 mmol, 2.3 equiv.), [Pd (allyl)Cl]₂ (1.0 mmol, 1.0 equiv.), K₂CO₃ (4.6 mmol, 4.6 equiv.) in acetone was stirred at 60°C for 24 h. Volatiles were removed *in vacuo*, and the crude product was purified by silica gel column (PE/AcOEt = 9:1) to afford the expected NHC-palladium complex.

2.1.1 | Chloro (allyl)[3-(2-isopropylphenyl)-1-(2,6-diisopropylphenyl)-4,4-dimethylimidazolidin-2-ylidene] palladium (II) **4a**

According to the general Procedure A, from imidazolium tetrafluoroborate **12a** (100 mg, 0.215 mmol, 2.3

equiv.), [Pd (allyl)Cl]₂ (38 mg, 0.103 mmol, 1 equiv.), and K₂CO₃ (0.43 mmol, 4.6 equiv.) the expected NHC-palladium complex **4a** was isolated as white solid (108 mg, 90% yield). Mp = 201.0–203.8°C (decomposition). In CDCl₃ (25°C) this complex exists as two isomers in a 2.3:1 ratio (unassigned). ¹H NMR chemical shifts that differ between two isomers will be denoted by (*maj*) and (*min*). ¹H NMR (400 MHz, CDCl₃) δ = 7.84 (d, J [H,H] = 7.9 Hz, 0.24H, H^{Ar} *min*), 7.57 (d, J [H,H] = 7.8 Hz, 0.68H, H^{Ar} *maj*), 7.32–7.22 (m, 3H, H^{Ar}), 7.21–7.13 (m, 2H, H^{Ar}), 7.12–7.06 (m, 1H, H^{Ar}), 4.65 (sept, J [H,H] = 7 Hz, 0.7H, H^{allyl} *maj*), 4.51 (sept, J [H,H] = 7.4 Hz, 0.26H, H^{allyl} *min*), 3.88 (d, J [H,H] = 10.4 Hz, 0.7H, H^{allyl} *maj*), 3.82–3.67 (m, 3H, CH₂ and CH [CH₃]₂), 3.66–3.56 (m, 0.3H, H^{allyl} *min*), 3.33–3.23 (m, 0.3H, CH [CH₃]₂ *min*), 3.22–3.09 (m, 1.75H, CH [CH₃]₂ *maj*), 3.05 (d, J [H,H] = 5.4 Hz, 0.7H, H^{allyl} *maj*), 2.94 (d, J [H,H] = 6.2 Hz, 0.3H, H^{allyl} *min*), 2.68–2.57 (m, 1H, H^{allyl}), 1.52 (m, 3H, CH₃), 1.39–1.29 (m, 6H, CH₃), 1.28–1.21 (m, 9H, CH₃), 1.21–1.17 (m, 1H, H^{allyl}), 1.17–1.12 (m, 6H, CH₃). ¹³C NMR (101 MHz, CDCl₃) δ = 213.6 (NCN *min*), 210.0 (NCN *maj*), 148.7 (C *maj*), 148.1 (C *min*), 148.0 (C *maj*), 147.7 (C *min*), 146.6 (C *maj*), 146.4 (C *min*), 136.3 (C *maj*), 136.0 (C *min*), 135.2 (C *min*), 134.2 (C *maj*), 133.9 (CH *min*), 133.4 (CH *maj*), 129.1 (CH *min*), 128.9 (CH *maj*), 126.2 (CH *min*), 126.0 (CH *maj*), 125.7 (CH *min*), 125.4 (CH *maj*), 124.7 (CH *min*), 124.6 (CH *maj*), 123.7 (CH *min*), 123.6 (CH *maj*), 114.4 (CH *maj*), 114.2 (CH *min*), 73.2 (CH₂ *maj*), 72.1 (CH₂ *min*), 67.5 (C), 67.0 (CH₂ *min*), 66.9 (CH₂ *maj*), 50.0 (CH₂ *min*), 49.7 (CH₂ *maj*), 31.6 (CH₂), 29.2 (CH₃ *maj*), 28.4 (CH *maj*), 28.3 (CH *min*), 28.2 (CH *maj*), 28.1 (CH *min*), 28.0 (CH *min*), 27.9 (CH *maj*), 26.9 (CH₃ *maj*), 26.6 (CH₃ *min*), 26.5 (CH₃ *maj*), 26.3 (CH₃ *min*), 25.7 (CH₃ *maj*), 25.5 (CH₃ *min*), 24.2 (CH₃ *min*), 24.1 (CH₃ *maj*), 24.0 (CH₃ *maj*), 23.4 (CH₃ *min*), 23.2 (CH₃ *maj*), 22.6 (CH₂), 14.1 (CH₃ *maj*). HRMS (ESI): m/z : 583.1886 calcd for: C₂₉H₄₁ClN₂PdNa⁺ [M]⁺; found: 583.1890. IR (ATR): 3036, 2965, 2929, 2868, 1588, 1468, 1448, 1429, 1405, 1384, 1367, 1331, 1303, 1290, 1266, 1238, 1215, 1178, 1092, 1055, 1033, 1019, 1001, 974, 956, 931, 877, 863, 805, 786, 760, 730, 699, 647, 623, 600, 576, 535 cm^{–1}. Chiral HPLC analysis: Lux-i-Amylose-3 column with a UV and CD detector at λ = 254 nm; flow rate 1 ml/min; eluent: hexane/*i*PrOH/DCM 80:10:10; 1st enantiomer: Rt = 6.83 min and 2nd enantiomer: Rt = 9.47 min.

2.1.2 | Chloro (allyl)[3-(2-benzhydrylphenyl)-1-(2,6-diisopropylphenyl)-4,4-dimethylimidazolidin-2-ylidene] palladium (II) **4c**

According to the general Procedure A, from imidazolium tetrafluoroborate **12c** (100 mg, 0.17 mmol, 2.3

equiv.), [Pd (allyl)Cl]₂ (30 mg, 0.08 mmol, 1 equiv.), and K₂CO₃ (47 mg, 0.34 mmol, 4.6 equiv.) the expected NHC-palladium complex **4c** was isolated as white solid (90 mg, 82% yield). Mp = 216.0°C (decomposition). In CDCl₃ (25°C) this complex exists as two isomers in a 2.6:1 ratio (unassigned). ¹H NMR chemical shifts that differ between two isomers will be denoted by (*maj*) and (*min*). ¹H NMR (400 MHz, CDCl₃): δ 8.00 (dd, *J* [H,H] = 7.4, 2.0 Hz, 0.3H, *H*^{Ar} *min*), 7.85 (dd, *J* [H,H] = 7.9, 1.5 Hz, 0.7H, *H*^{Ar} *maj*), 7.38–7.27 (m, 7H, *H*^{Ar}), 7.23–7.12 (m, 7H, *H*^{Ar}), 7.03 (dd, *J* [H,H] = 7.6, 1.9 Hz, 0.7H, *H*^{Ar}, *min*), 6.97 (d, *J* [H,H] = 6.8 Hz, 1.4H, *H*^{Ar}, *maj*), 6.24 (s, 0.3H, CH [Ph]₂ *min*), 6.13 (s, 0.7H, CH [Ph]₂ *maj*), 4.81–4.64 (m, 0.7H, *H*^{allyl} *maj*), 4.47–4.37 (m, 0.3H *H*^{allyl} *min*), 4.06–3.93 (m, 1H, *H*^{allyl}), 3.63–3.53 (m, 2H, *H*^{allyl} and CH₂), 3.65–3.51 (m, 1H, CH₂), 3.30–3.16 (m, 1H, *H*^{allyl}), 2.85–2.69 (m, 1.7H, CH [CH₃]₂), 2.54 (d, *J* (H,H) = 6.8 Hz, 0.3H CH (CH₃)₂ *min*), 1.69–1.63 (m, 3H, CH₃), 1.54 (s, 4H, CH₃), 1.43 (dd, *J* (H,H) = 6.7, 1.6 Hz, 4H, CH (CH₃)₂ *maj*), 1.41–1.37 (m, 1.7H, CH (CH₃)₂ *min*), 1.33–1.28 (m, 4.3H, CH₃), 1.28–1.26 (m, 1H, *H*^{allyl}), 1.23–1.13 (m, 4.3H, CH₃), 0.78 (s, 0.8H, CH₃ *min*), 0.54 (s, 2H, CH₃ *maj*). ¹³C NMR (101 MHz, CDCl₃): δ = 212.4 (NCN *min*), 209.8 (NCN *maj*), 148.8 (C *maj*), 148.3 (C *min*), 146.1 (C *maj*), 145.8 (C *min*), 144.7 (C *maj*), 144.2 (C *min*), 143.1 (C *min*), 142.6 (C *maj*), 142.5 (C *maj*), 142.4 (C, *min*), 137.7 (C *min*), 137.1 (C *maj*), 136.5 (C *maj*), 136.1 (C, *min*), 133.3 (CH), 132.8 (CH), 131.8 (CH), 131.7 (CH), 129.9 (CH), 129.8 (CH), 129.5 (CH), 129.2 (CH), 129.0 (CH), 128.5 (CH), 128.3 (CH), 128.2 (CH), 128.11 (CH), 128.08 (CH), 127.8 (CH), 126.7 (CH), 126.6 (CH), 126.5 (CH), 126.3 (CH), 126.2 (CH), 124.8 (CH), 124.7 (CH), 123.7 (CH), 123.5 (CH), 115.2 (CH), 114.7 (CH), 74.1 (CH₂ *maj*), 72.1 (CH₂ *min*), 68.4 (C *min*), 68.2 (C *maj*), 67.0 (CH₂ *min*), 66.8 (CH₂ *maj*), 50.4 (CH *min*), 50.2 (CH *maj*), 49.8 (CH₂ *min*), 49.15 (CH₂ *maj*), 31.6 (CH₂ *maj*), 29.8 (CH₃ *maj*), 29.4 (CH₃ *min*), 28.4 (CH *maj*), 28.3 (CH *min*), 28.1 (CH *maj*), 27.1 (CH₃ *maj*), 26.9 (CH₃ *min*), 26.4 (CH₃ *maj*), 25.4 (CH₃ *min*), 25.0 (CH₃ *maj*), 23.9 (CH₃ *maj*), 23.8 (CH₃ *min*), 23.3 (CH₃ *maj*), 22.6 (CH₂), 14.1 (CH₃). HRMS (ESI): *m/z*: 705.2210 calcd for: C₃₉H₄₅ClN₂PdNa⁺ [M]⁺; found: 705.2206. IR (ATR): 2963, 2925, 2864, 1596, 1493, 1476, 1463, 1445, 1425, 1397, 1384, 1369, 1327, 1301, 1257, 1215, 1172, 1097, 1076, 1054, 1039, 1021, 1002, 933, 897, 871, 847, 815, 782, 769, 761, 753, 740, 706, 647, 620, 601, 544, 517 cm⁻¹. Chiral HPLC analysis: Chiralpak IG column with a UV and CD detector at λ = 254 nm; flow rate 1 ml/min; eluent: heptane/*i*PrOH/DCM 70:10:20; 1st enantiomer: Rt = 4.71 min and 2nd enantiomer: Rt = 6.04 min.

2.1.3 | (1-(2,6-Diisopropylphenyl)-3-(2-isopropylphenyl)-4,4-dimethylimidazolidin-2-ylidene)copper(I) chloride **5a**

1-(2,6-Diisopropylphenyl)-3-(2-isopropylphenyl)-4,4-dimethylimidazolidinium tetrafluoroborate **12a** (470 mg, 1 mmol) was suspended in MeOH (20 ml). Dowex-22 Cl (1.1 g) were added in the mixture and the reaction was stirred at 25°C for 24 h. The solvent was removed under vacuum. The residue was dissolved in dichloromethane (20 ml), dried by Na₂SO₄ and filtered. The solvent was removed under vacuum to give the imidazolinium chloride which is directly used without further purification. A mixture of 1-(2,6-diisopropylphenyl)-3-(2-isopropylphenyl)-4,4-dimethylimidazolidinium chloride (200 mg, 0.5 mmol), CuCl (53 mg, 0.55 mmol, 1.1 equiv.), K₂CO₃ (135 mg, 1 mmol, 2.0 equiv.) in acetone (10 ml) was stirred at 60°C for 20 h. The reaction mixture was filtered through a Celite[®] pad and the solvent was removed under vacuum. The crude product was triturated with pentane (5 ml) and the brown solid was filtrated off to give the NHC-copper complex. (109 mg, 47% yield). R_f = 0.50 (EP/Et₂O 1:1). Mp = 214.7–216.0°C. ¹H NMR (300 MHz CDCl₃) δ = 7.46–7.37 (m, 3H, *H*^{Ar}), 7.28–7.23 (m, 6H, *H*^{Ar}), 3.79 (s, 2H, CH₂), 3.26 (sept, *J* (H,H) = 6.9 Hz, 1H, CH (CH₃)₂), 3.13 (sept, *J* (H,H) = 6.9 Hz, 1H, CH (CH₃)₂), 3.08 (sept, *J* (H,H) = 6.9 Hz, 1H, CH (CH₃)₂), 1.60 (s, 3H, C (CH₃)₂), 1.40 (dd, *J* (H,H) = 6.8 and 4.7 Hz, 6H, CH (CH₃)₂), 1.38–1.32 (m, 16H, CH (CH₃)₂ and C (CH₃)₂). ¹³C NMR (75 MHz, CDCl₃) δ = 202.1 (C), 148.2 (C), 146.7 (C), 146.7 (C), 134.6 (C), 134.1 (C), 130.4 (CH), 129.72 (CH), 129.68 (CH), 127.3 (CH), 126.5 (CH), 124.6 (CH), 124.5 (CH), 67.2 (C), 66.9 (CH₂), 29.1 (CH₃), 28.8 (CH), 28.5 (CH), 28.4 (CH), 26.3 (CH₃), 26.2 (CH₃), 25.4 (CH₃), 25.1 (CH₃), 24.3 (CH₃), 23.9 (CH₃), 23.4 (CH₃). HRMS (ESI): *m/z*: 497.1755 calcd for: C₂₆H₃₆ClCuN₂Na⁺ [M + Na]⁺; found 497.1754. IR (ATR): 2957, 2928, 2866, 1481, 1469, 1449, 1414, 1385, 1368, 1330, 1312, 1291, 1265, 1255; 1216, 1173, 1093, 1055, 1031, 935, 869, 810, 786, 767, 760, 739, 649, 613; 600, 534 cm⁻¹. Chiral HPLC analysis: Chiralpak IG column with a UV and CD detector at λ = 254 nm; flow rate 1 ml/min; eluent: heptane/EtOH/DCM 80:10:10; 1st enantiomer: Rt = 5.93 min and 2nd enantiomer: Rt = 7.01 min.

2.1.4 | 3-(2-Benzhydrylphenyl)-1-(2,6-diisopropylphenyl)-4,4-dimethylimidazolidin-2-ylidene)copper(I) chloride **5c**

A mixture of 3-(2-benzhydrylphenyl)-1-(2,6-diisopropylphenyl)-4,4-dimethyl-4,5-dihydro-1*H*-imidazol-3-

ium chloride **12c'** (234 mg, 0.44 mmol), CuCl (48 mg, 0.48 mmol, 1.1 equiv.), K₂CO₃ (120 mg, 0.9 mmol, 2.0 equiv.) in acetone (5 ml) was stirred at 60°C for 20 h. The reaction mixture was filtered through a Celite® pad and the solvent was removed under vacuum. The crude product was triturated with pentane (5 ml) and the brown solid was filtrated off to give the NHC-copper complex. (87 mg, 33% yield). R_f = 0.44 (EP/Et₂O 1:1). Mp = 270.0°C (decomposition). ¹H NMR (300 MHz CDCl₃) δ = 7.38–7.30 (m, 5H, H^{Ar}), 7.26–7.14 (m, 12H, H^{Ar}), 6.10 (s, 1H, CHPh₂), 3.62 (d, *J*(H,H) = 1.6 Hz, 2H, CH₂), 3.20 (sept, *J*(H,H) = 6.8 Hz, 1H, CH (CH₃)₂), 3.04 (sept, *J*(H,H) = 6.6 Hz, 1H, CH (CH₃)₂), 1.58 (s, 3H, C (CH₃)₂), 1.39–1.28 (m, 12H, CH (CH₃)₂), 0.84 (s, 3H, C (CH₃)₂). ¹³C NMR (75 MHz, CDCl₃) δ = 146.6 (C), 146.4 (C), 143.5 (C), 142.8 (C), 142.5 (C), 136.4 (C), 134.6 (C), 132.7 (CH), 131.1 (CH), 129.8 (CH), 129.7 (CH), 129.6 (CH), 129.1 (CH), 128.7 (CH), 128.6 (CH), 127.5 (CH), 126.7 (CH), 126.6 (CH), 124.8 (CH), 124.4 (CH), 68.1 (C), 67.0 (CH₂), 50.6 (CH), 29.3 (CH₃), 28.7 (CH), 28.6 (CH), 26.0 (CH₃), 25.4 (CH₃), 25.1 (CH₃), 24.7 (CH₃), 23.8 (CH₃). HRMS (ESI): *m/z*: 621.2068 calcd for: C₃₆H₄₀ClCuN₂Na⁺ [M + Na]⁺; found 621.2075. IR (ATR): 2961, 2925, 2865, 1685, 1597, 1480, 1468, 1447, 1405, 1386, 1368, 1332, 1315, 1292, 1259, 1242, 1218, 1178, 1096, 1078, 1056, 1028, 806, 763, 751, 733, 700, 618, 603, 590, 541 cm⁻¹. Chiral HPLC analysis: Chiralpak IH column with a UV and CD detector at λ = 254 nm; flow rate 1 ml/min; eluent: heptane/*i*PrOH/DCM 90:5:5; 1st enantiomer: Rt = 6.74 min and 2nd enantiomer: Rt = 9.51 min.

2.1.5 | 1-(2,6-Diisopropylphenyl)-3-(2,6-diisopropylphenyl)-4,4-dimethylimidazolidin-2-ylidene)silver(I) chloride **6a**

1-(2,6-Diisopropylphenyl)-3-(2-isopropylphenyl)-4,4-dimethylimidazolidinium chloride **12a'** (1 equiv, 100 mg, 0.24 mmol) was suspended in 3 ml of CH₃CN (dried over 4-Å molecular sieves), then Ag₂O (5 equiv, 280 mg, 1.32 mmol) was added and the reaction mixture was stirred at 60°C for 1 h. After filtration on Celite® pad and removing the solvent, a yellow precipitate was obtained and then purified by silica gel chromatography with DCM as eluent. The title NHC-silver complex was obtained as a yellow solid (85 mg, 68% yield). Mp = 156°C (decomposition). ¹H NMR (400 MHz, CDCl₃): δ = 7.38–7.29 (m, 3H, H^{Ar}), 7.21–7.12 (m, 4H, H^{Ar}), 3.74 (s, 2H, CH₂), 3.21–3.09 (m, 1H, CH (CH₃)₂), 3.13–2.99 (m, 1H, CH (CH₃)₂), 3.00–2.89 (m, 1H, CH (CH₃)₂), 1.53 (s, 3H, CH₃), 1.38–1.20 (m, 21H, CH₃ and CH (CH₃)₂). ¹³C NMR (101 MHz, CDCl₃): δ = 206.9 (d, *J*^I[¹⁰⁹Ag–¹³C] = 258.7 Hz, NCN), 206.9 (d, *J*^I[¹⁰⁷Ag–¹³C] = 223.7 Hz, NCN), 148.1 (C), 146.6 (C), 146.6 (C), 134.7 (C), 134.3 (C),

130.3 (CH), 129.9 (CH), 129.9 (CH), 127.5 (CH), 126.6 (CH), 124.8 (CH), 124.6 (CH), 67.38 (d, *J*³[¹⁰⁹Ag–¹³C] = 80.9 Hz, CH₂), 67.38 (d, *J*³[¹⁰⁷Ag–¹³C] = 64.5 Hz, CH₂). 29.2 (CH₃), 28.7 (CH), 28.5 (CH), 28.4 (CH), 26.4 (CH₃), 26.3 (CH₃), 25.4 (CH₃), 25.1 (CH₃), 24.4 (CH₃), 24.0 (CH₃), 23.4 (CH₃). HRMS (ESI): *m/z*: 520.1615 calcd for: C₂₆H₃₆AgClN₂⁺ [M⁺]; found: 520.1610. IR (ATR): 3067, 2961, 2925, 2867, 1718, 1677, 1590, 1483, 1451, 1416, 1385, 1366, 1330, 1309, 1291, 1266, 1240, 1216, 1176, 1091, 1055, 1033, 975, 956, 934, 862, 806, 785, 760, 737, 648, 599, 574, 532 cm⁻¹. Chiral HPLC analysis: Chiralpak IG column with a UV and CD detector at λ = 254 nm; flow rate 1 ml/min; eluent: heptane/ethanol/dichloromethane (80/10/10); 1st enantiomer: Rt = 7.55 min and 2nd enantiomer: Rt = 8.83 min.

2.1.6 | 1-(2,6-Diisopropylphenyl)-3-(2,6-diisopropylphenyl)-4,4-dimethylimidazolidin-2-ylidene)gold(I) chloride **7a**

A mixture of 1-(2,6-diisopropylphenyl)-3-(2-isopropylphenyl)-4,4-dimethylimidazolidinium chloride **12a'** (90 mg, 0.22 mmol), [Au (DMS)Cl] (64 mg, 0.22 mmol, 1 equiv.), K₂CO₃ (30 mg, 0.22 mmol, 1 equiv.) in acetone (3 ml) was stirred at 60°C for 24 h. The reaction mixture was filtered through a Celite® pad and the solvent was removed under vacuum. The crude product was purified by silica gel chromatography with DCM to give the NHC-gold complex as white solid. (108 mg, 81% yield). Mp = 230.9–232.0°C. ¹H NMR (400 MHz, CDCl₃) δ = 7.47–7.43 (m, 2H, H^{Ar}), 7.40 (t, *J*(H,H) = 7.8 Hz, 1H, H^{Ar}), 7.27–7.23 (m, 3H, H^{Ar}), 7.22 (q, *J*(H,H) = 1.5 Hz, 1H, H^{Ar}), 3.78 (s, 2H, CH₂), 3.28–3.09 (m, 2H, CH (CH₃)₂), 3.02 (sept, *J*(H,H) = 6.9 Hz, 1H, CH (CH₃)₂), 1.61 (s, 3H, CH₃), 1.51–1.42 (m, 6H, CH (CH₃)₂), 1.42–1.36 (m, 6H, CH (CH₃)₂), 1.36–1.30 (m, 9H, CH (CH₃)₂ and CH₃). ¹³C NMR (101 MHz, CDCl₃) δ = 194.7 (NCN), 148.3 (C), 146.7 (C), 146.6 (C), 134.3 (C), 133.7 (C), 130.4 (CH), 129.9 (CH), 129.9 (CH), 127.3 (CH), 126.5 (CH), 124.7 (CH), 124.5 (CH), 67.0 (C), 66.8 (CH₂), 29.0 (CH₃), 28.8 (CH₃), 28.6 (CH), 28.5 (CH), 26.3 (CH), 26.0 (CH₃), 25.1 (CH₃), 24.9 (CH₃), 24.5 (CH₃), 24.0 (CH₃), 23.4 (CH₃). HRMS (ESI): *m/z*: 631.2125 calcd for: C₂₆H₃₆ClN₂AuNa⁺ [M + Na]⁺; found: 631.2124. IR (ATR): 3048, 2962, 2927, 2868, 1590, 1488, 1461, 1426, 1386, 1368, 1335, 1317, 1293, 1267, 1242, 1218, 1177, 1092, 1055, 1033, 979, 935, 892, 868, 806, 789, 760, 732, 670, 650, 633, 600, 575, 533 cm⁻¹. Chiral HPLC analysis: Lux-i-Amylose-3 column with a UV and CD detector at λ = 254 nm; flow rate 1 ml/min; eluent: heptane/ethanol/dichloromethane (80/10/10); 1st enantiomer: Rt = 5.74 min and 2nd enantiomer: Rt = 6.36 min.

2.1.7 | Chloro(dmba)[3-(2-benzhydrylphenyl)-1-(2,6-diisopropylphenyl)-4,4-dimethylimidazolidin-2-ylidene] palladium (II) **15c**

In a 10-ml Schlenk tube, PdCl₂ (48 mg, 0.16 mmol, 1 equiv.) and 250 mg of 4-Å molecular sieves were charged as well as 3 ml of dry CH₃CN. Then, dimethylbenzylamine (26 µl, 0.17 mmol, 1.05 equiv.) was added and the reaction mixture was stirred at 80°C for 30 minutes. Cs₂CO₃ (138.5 mg, 0.43 mmol, 2.5 equiv.) was added and the stirring was prolonged for 30 min at 80°C. Imidazolinium tetrafluoroborate **12c** (100 mg, 0.17 mmol, 1.05 equiv.) was added and reaction mixture was heated at 80°C for 16 h. The reaction mixture was cooled to room temperature, filtered through a short Celite® pad and volatiles were removed. Purification by silica gel chromatography (PE/EtOAc = 8:2) gave the expected NHC-palladacycle **15c** as white solid (55 mg, 44% yield). Mp = 141.1–142.8°C. In CDCl₃ (25°C) this complex exists as two isomers in a 7.5:1 ratio (unassigned). ¹H NMR chemical shifts that differ between two isomers will be denoted by (*maj*) and (*min*). ¹H NMR (500 MHz, CDCl₃) δ = 8.00 (dd, *J*(H,H) = 8.1, 1.4 Hz, 0.12H, *H*^{Ar} *min*), 7.60–7.56 (m, 0.12H, *H*^{Ar} *min*), 7.52–7.42 (m, 4H, *H*^{Ar}), 7.38–7.29 (m, 6H, *H*^{Ar}), 7.27–7.19 (m, 4H, *H*^{Ar}), 7.18–7.12 (m, 3H, *H*^{Ar}), 7.12–7.02 (m, 2H, *H*^{Ar}), 6.98–6.84 (m, 4H, *H*^{Ar}), 6.83–6.77 (m, 1.4H, *H*^{Ar}), 6.75–6.70 (m, 0.24H, *H*^{Ar} *min*), 6.54 (d, *J*(H,H) = 8.0 Hz, 0.24H, *H*^{Ar} *min*), 6.37 (s, 0.12H, *H*^{Ar} *min*), 4.13–4.05 (m, 0.16H, CH (CH₃)₂ *min*), 4.03–3.90 (m, 2H, CH (CH₃)₂ and CH₂^{Backbone} *maj*), 3.86 (d, *J*(H,H) = 10.3 Hz, 1H, CH₂^{benzyl} *maj*), 3.82 (d, *J*(H,H) = 10.3 Hz, 0.17H, CH₂^{benzyl} *min*), 3.74–3.62 (m, 0.31H, CH₂^{Backbone} *min*), 3.49–3.38 (m, 2H, CH (CH₃)₂ and CH₂^{Backbone} *maj*), 3.33 (d, *J*(H,H) = 13.6 Hz, 0.16H, CH₂^{benzyl} *min*), 3.23 (d, *J*(H,H) = 13.6 Hz, 1H, CH₂^{benzyl} *maj*), 2.59 (s, 3H, N (CH₃)₂ *maj*), 2.48 (s, 0.4H, N (CH₃)₂ *min*), 2.34 (s, 0.4H, N (CH₃)₂ *min*), 2.27 (s, 3H, N (CH₃)₂ *maj*), 1.75 (d, *J*(H,H) = 6.4 Hz, 3H, CH (CH₃)₂ *maj*), 1.68 (s, 3H, CH₃ *maj*), 1.60 (d, *J*(H,H) = 6.5 Hz, 0.4H, CH (CH₃)₂ *min*), 1.52 (s, 0.4H, CH₃ *min*), 1.37 (s, 0.4H, CH₃ *min*), 1.20 (d, *J*(H,H) = 6.8 Hz, 3H, CH (CH₃)₂ *maj*), 1.17 (d, *J*(H,H) = 7.0 Hz, 0.6H, CH (CH₃)₂ *min*), 1.14 (d, *J*(H,H) = 6.9 Hz, 3H, CH (CH₃)₂ *maj*), 0.90 (d, *J*(H,H) = 6.6 Hz, 3.8H, CH (CH₃)₂), 0.71 (d, *J*(H,H) = 6.6 Hz, 0.3H, CH (CH₃)₂ *min*), 0.67 (s, 0.3H, CH₃ *min*), 0.20 (s, 3H, CH₃ *maj*). ¹³C APT NMR (126 MHz, CDCl₃) δ = 200.2 (NCN), 150.8 (C), 148.0 (C), 147.8 (C), 146.3 (C), 146.1 (C), 144.9 (C), 142.9 (C), 137.9 (C), 136.9 (C), 136.4 (CH), 133.0 (CH), 130.9 (CH), 130.6 (CH), 130.0 (CH), 129.9 (CH), 129.8 (CH), 129.0 (CH), 128.6 (CH), 128.2 (CH), 127.5 (CH), 127.4 (CH), 127.1 (CH), 126.5 (CH), 125.6 (CH),

125.3 (CH), 124.5 (CH), 124.4 (CH), 123.6 (CH), 123.2 (CH), 121.7 (CH), 72.3 (CH₂), 67.6 (CH₂), 66.9 (CH₂), 50.8 (CH), 49.6 (CH₃), 49.5 (CH₃), 29.4 (CH₃), 28.1 (CH), 27.1 (CH), 26.5 (CH₃), 25.6 (CH₃), 24.0 (CH₃), 22.8 (CH₃). HRMS (ESI): *m/z*: 798.2790 calcd for: C₄₅H₅₂ClN₃PdNa⁺ [M + Na]⁺; found: 798.2801. IR (ATR): 3059, 2966, 2924, 2869, 1736, 1598, 1582, 1493, 1464, 1443, 1422, 1385, 1369, 1330, 1310, 1266, 1216, 1175, 1100, 1077, 1047, 1027, 996, 975, 931, 888, 866, 849, 802, 781, 757, 731, 702, 657, 645, 607, 545, 525 cm⁻¹. Chiral HPLC analysis: Chiralpak IG column with a UV and CD detector at λ = 254 nm; flow rate 1 ml/min; eluent: heptane/EtOH/DCM 90:5:5; 1st enantiomer: Rt = 4.83 min and 2nd enantiomer: Rt = 6.19 min.

2.1.8 | Chloro(1,5-cyclooctadiene)[3-(2-benzhydrylphenyl)-1-(2,6-diisopropylphenyl)-4,4-dimethylimidazolidin-2-ylidene] palladium (II) **16c**

A mixture of chloro(1,5-cyclooctadiene)rhodium(I) dimer (40 mg, 0.08 mmol, 1.1 equiv), imidazolinium tetrafluoroborate **12c** (100 mg, 0.17 mmol, 2.3 equiv.) and K₂CO₃ (47 mg, 0.34 mmol, 4.6 equiv.) in acetone was stirred at 60°C for 20 h. The reaction mixture was cooled to room temperature, filtered through a Celite® pad and volatiles were removed *in vacuo*. After purification by silica gel chromatography (PE/DCM 1:1), the title rhodium complex was obtained as a yellow crystalline powder (102 mg, 85%). Mp = 112.7–115.0°C (decomposition). In CDCl₃ (25°C) the complex exists as two isomers in a 5.7:1 ratio (unassigned). ¹H NMR chemical shifts that differ between two isomers will be denoted by (*maj*) and (*min*). ¹H NMR (500 MHz, CDCl₃) δ = 8.53 (d, *J*(H,H) = 7.9 Hz, 0.8H, *H*^{Ar} *maj*), 7.62 (d, *J*(H,H) = 7.4 Hz, 0.2H, *H*^{Ar} *min*), 7.50–7.34 (m, 5H, *H*^{Ar}), 7.33–7.17 (m, 9H, *H*^{Ar}), 7.13 (d, *J*(H,H) = 7.4 Hz, 1.8H, *H*^{Ar} *maj*), 7.01 (d, *J*(H,H) = 7.8 Hz, 0.2H, *H*^{Ar} *min*), 5.83 (s, 1H, CHPh₂), 4.80–4.69 (m, 0.25H, CH=CH^{COD} *min*), 4.61 (m, 1.65H, CH=CH^{COD} *maj*), 4.33 (sept, *J*(H,H) = 6.8 Hz, 0.85H, COD *maj*), 4.03 (sept, *J*(H,H) = 6.7 Hz, 0.15H, COD *min*), 3.65 (d, *J*(H,H) = 10.0 Hz, 1H, CH₂^{backbone}), 3.56 (s, 0.3H, COD *min*), 3.40 (d, *J*(H,H) = 10.1 Hz, 1H, CH₂^{backbone}), 3.29–3.21 (m, 1H, COD), 3.11–2.95 (m, 1.85H, CH (CH₃)₂ *maj*), 2.23–2.15 (m, 0.15H, CH (CH₃)₂ *min*), 1.89–1.76 (m, 1H, COD), 1.60 (s, 4H, CH₃), 1.55 (d, *J*(H,H) = 6.6 Hz, 3H, CH (CH₃)₂), 1.44–1.25 (m, 11H, CH (CH₃)₂ and COD), 1.21 (d, *J*(H,H) = 6.8 Hz, 0.4H, CH (CH₃)₂ *min*), 1.17 (d, *J*(H,H) = 6.9 Hz, 2.4H, CH (CH₃)₂ *maj*), 1.15–1.07 (m, 2H, COD), 0.67 (s, 0.3H, CH₃ *min*), 0.54 (s, 2.5H, CH₃ *maj*). ¹³C APT NMR (126 MHz, CDCl₃) δ = 216.3 (d, *J*¹[¹⁰³Rh–¹³C] = 47.9 Hz, NCN), 149.8 (C), 149.7 (C), 146.9 (C), 146.2 (C), 146.0 (C),

145.1 (C), 144.4 (C), 144.2 (C), 143.8 (C), 142.0 (C), 139.0 (C), 138.2 (C), 136.8 (C), 136.6 (C), 135.9 (C), 134.3 (CH), 133.8 (CH), 131.4 (CH), 131.0 (CH), 130.5 (CH), 130.0 (CH), 129.8 (CH), 129.2 (CH), 128.5 (CH), 128.3 (CH), 128.2 (CH), 127.9 (CH), 127.2 (CH), 126.8 (CH), 126.7 (CH), 126.5 (CH), 126.2 (CH), 125.6 (CH), 125.6 (CH), 125.3 (CH), 125.0 (CH), 123.6 (CH), 123.2 (CH), 97.3 (CH₂), 97.3 (CH₂), 97.0 (CH₂), 96.9 (CH₂), 68.5 (CH₂), 68.4 (CH₂), 67.9 (C), 67.1 (C), 66.1 (CH₂), 66.0 (CH₂), 51.1 (CH₂), 49.7 (CH₂), 32.9 (CH₃), 31.8 (CH₃), 31.7 (CH₃), 28.9 (CH), 28.8 (CH₃), 28.4 (CH), 28.2 (CH), 27.7 (CH), 27.5 (CH₃), 26.6 (CH), 24.5 (CH), 24.3 (CH), 23.3 (CH), 22.8 (CH₃), 14.3 (CH). HRMS (ESI): *m/z*: 769.2766 calcd for: C₄₄H₅₂ClN₂RhNa⁺ [M + Na]⁺; found: 769.2771. IR (ATR): 3060, 3026, 2964, 2932, 2873, 2828, 1598, 1493, 1467, 1444, 1412, 1383, 1368, 1327, 1299, 1279, 1265, 1239, 1214, 1199, 1173, 1113, 1095, 1078, 1055, 1033, 993, 972, 957, 932, 887, 868, 805, 781, 758, 731, 700, 641, 620, 605, 544 cm⁻¹. Chiral HPLC analysis: Chiralpak ID column with a UV detector at λ = 220 nm and CD detector at λ = 254 nm; flow rate 1 ml/min; eluent: heptane/EtOH/DCM 80:10:10; 1st enantiomer: Rt = 5.56 min and 2nd enantiomer: Rt = 6.33 min.

3 | RESULTS AND DISCUSSION

3.1 | Theoretical calculations

We commenced our study with Density Functional Theory (DFT) calculations in order to anticipate the configurational stability of complexes bearing the saturated NHC possessing a *gem* dimethyl pattern. Whereas the rotational barrier value should be higher than 93 kJ·mol⁻¹; (*t*_{1/2} > 1000 s at 25°C) to observe atropisomers, we targeted enantiomerization barriers (Δ*G*[‡]) above 110 kJ·mol⁻¹ (*t*_{1/2} > 12 days at 25°C), in order to get enantiomers of metal complexes that could be separated by chiral HPLC in preparative scale. The results of DFT calculations have been gathered in Figure 3; rotations on the backbone side are noted Δ*G*[‡]_(BB) (red arrow) and rotations on the metal side are noted Δ*G*[‡]_(M) (M = Pd, Cu, Ag, Au) (blue arrow). Palladium and gold complexes **4a** and **7a** should present the expected configurational stability even if the direction of the most favorable rotation could not be unequivocally assigned because the values of Δ*G*[‡]_(M) and Δ*G*[‡]_(BB) were of the same magnitude. Of note, for palladium complex **4a**, two configurations of minimal energy were calculated. These configurations that differ from the allyl orientation were close in energy (4 kJ·mol⁻¹); the lowest minimum has been selected for the rotational barrier calculation. With copper(I) and silver(I), complexes **5a**

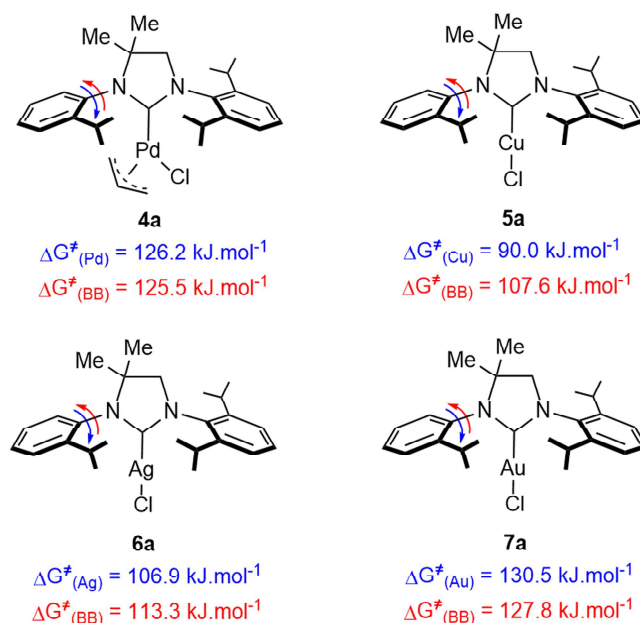


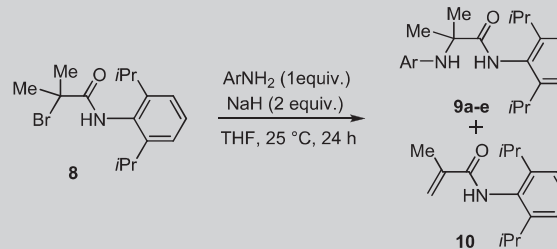
FIGURE 3 Determination of the rotational barrier values by DFT calculations (BB = backbone)

and **6a**, configuration stabilities should be significantly reduced and even if the observation of enantiomers by chiral HPLC analysis was expected, the isolation of enantiopure complexes by chPLC in a preparative scale might be troublesome. Theoretical calculations suggested that the more favorable rotation would take place on the metal side as it was concluded from our previous studies.^{22,23}

3.2 | Imidazolinium synthesis

Targeted imidazolinium salts, precursors of NHC ligands with a saturated backbone, were prepared according to the synthetic route reported by Grubbs.²⁶ Amide **8**, prepared from α-bromoisobutyryl bromide and 2,6-diisopropylaniline, was treated with several anilines in the presence of NaH to afford the expected **9a** (Table 1). Whereas, the substitution reaction was quantitative with 2-isopropylaniline (Entry 1), yields were lower with more sterically demanding anilines (Entries 2–5) and required prolonged reaction times (Entries 4 and 5). With bulky 2-*tert*-butylaniline, the by-product **10**, resulting from an elimination reaction, was isolated (Entry 2). The formation of this by-product was also observed in minute amounts with benzhydryl-containing anilines (Entries 3–5).

The reduction of amides **9** into diamines was found demanding and could be only achieved with borane THF complex at 60°C and prolonged reaction times (Table 2).

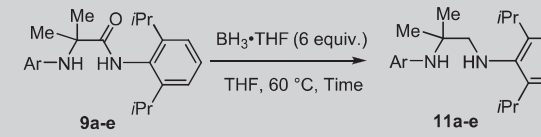
TABLE 1 Synthesis of amides **9**


Entry	Ar	9 (yield)	10 (yield)
1		9a (99%)	—
2		9b (53%)	10 (17%)
3		9c (64%)	10 (traces)
4 ^a		9d (90%)	10 (traces)
5 ^b		9e (72%)	10 (traces)

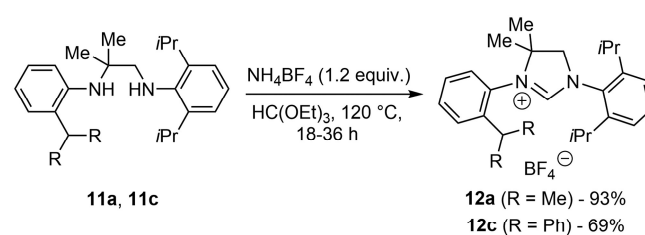
^aReaction time: 96 h.^bReaction time: 48 h.

Whereas diamines **11a** and **11c** were isolated in satisfactory yields (Entries 1 and 3), amides containing the bulkiest aryl substituents reacted hardly at all because some starting material was remaining after few days of reaction. Unfortunately, no desired product formation was observed, but only degradation products that included alkene **10** (Entries 2 and 4). Diamine **11e** was isolated but in low quantities which were insufficient to follow on the synthesis (Entry 5).

The treatment of diamines **9a** and **9c** with ammonium tetrafluoroborate in triethyl orthoformate at 120 °C gave the expected imidazolinium **12** as tetrafluoroborate salts with good to excellent yields (Scheme 1).

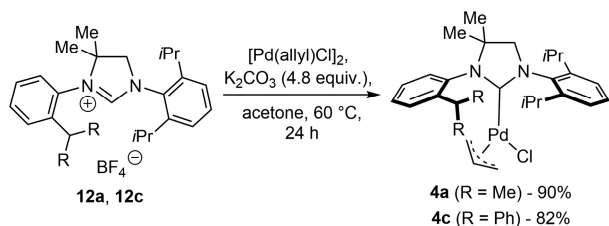
TABLE 2 Reduction of amides **9**


Entry	Ar	Time (h)	11 (yield)
1		48	11a (66%)
2		72	degradation
3		96	11c (78%)
4		96	degradation
5		96	11e (9%)

SCHEME 1 Synthesis of imidazolinium salts **12**

3.3 | Palladium complexes preparation, resolution by cHPLC, and characterization

With these two imidazolinium salts in hand, we undertook the synthesis of the corresponding palladium allyl complexes by treating **12a** and **12c** with [Pd(allyl)Cl]₂ and K₂CO₃ in acetone (Scheme 2). Both complexes **4a**



SCHEME 2 Preparation of chiral NHC-palladium complexes **4**

and **4c** were isolated in very good yield after silica gel chromatography. ^1H NMR spectroscopy showed the presence of two isomers in solution with a ratio ca. 70:30 for both complexes (For details, see supporting information). This observation was anticipated by theoretical calculations, for which two possible orientations have been identified for the allyl ligand. The low difference of energy between these two isomers ($4\text{ kJ}\cdot\text{mol}^{-1}$) led theoretically to a ratio of 83:17 at 25°C .

To our delight, both enantiomers of complexes **4a** and **4c** could be separated by chiral HPLC using Chiralpak IG and Lux-i-Amylose-3 columns (Figure 4). The resolution of these palladium complexes in preparative scale was

carried out with a 1-cm diameter Chiralpak IG column (For details, see supporting information). From 100 mg of **4a**, 44 mg of the first eluted enantiomer and 45 mg of the second eluted enantiomers were obtained with excellent enantiopurities ($>99\%$ ee). From 57 mg of complex **4c**, first and second eluted enantiomers were isolated enantiomerically pure ($>99.5\%$ ee) in 19- and 17-mg quantities, respectively. With good to excellent resolution yields (63% for **4c** and 89% for **4a**), resolution by chPLC in preparative scale proved to be an efficient process to obtain enantiomers with excellent enantiopurities.

Because we have planned to study the performances of complexes **4** in asymmetric catalysis, the determination of their absolute configuration was investigated. Unfortunately, attempts to grow suitable crystals for DRX failed. ECD spectra were recorded, and theoretical spectra were calculated by DFT and Time-Dependent Density Functional Theory (TD-DFT) taking into account both conformers resulting from the allyl orientation (For details, see supporting information). A good correlation between experimental and calculated UV and ECD spectra was observed, which allowed to determine the absolute configuration of the second eluted enantiomers on ChiralPak IG as **(R_a)-(+)-4a** and **(R_a)-(+)-4c** (Figure 5). Of note, DFT

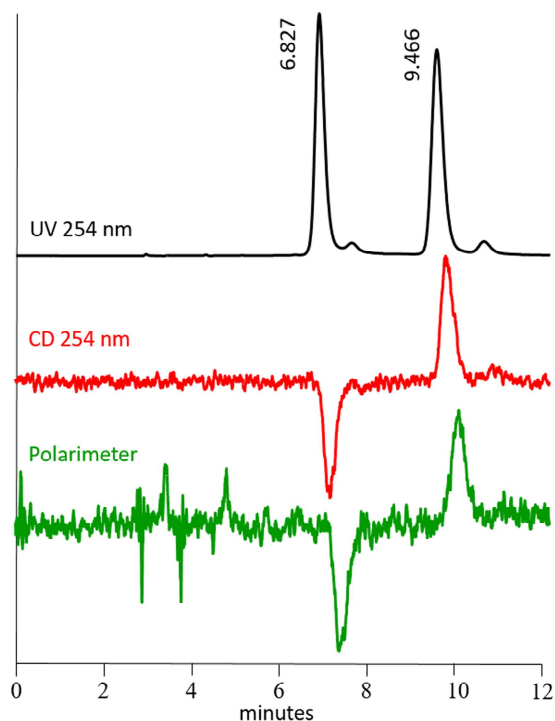


FIGURE 4 Separation of enantiomers of palladium complex **4a** on lux-i-Amylose-3 column; hexane/isopropanol/dichloromethane 80:10:10, 1 ml/min, 25°C ; top (black) UV detector at 254 nm; middle (red) CD detector at 254 nm; bottom (green) polarimeter

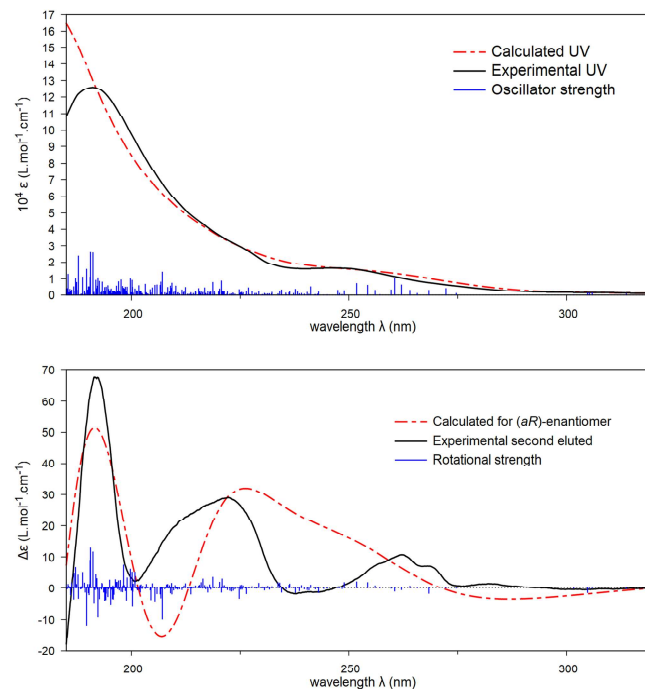


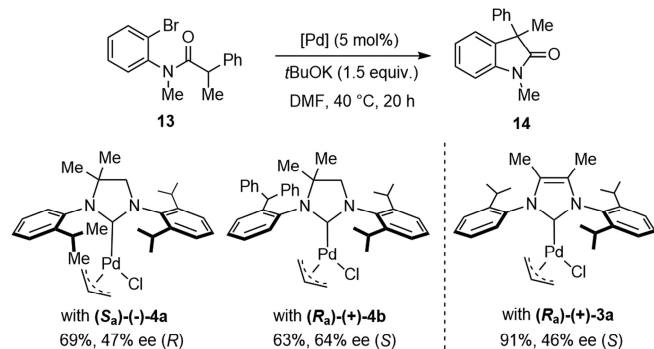
FIGURE 5 Comparison of UV (top) and electronic circular dichroism (ECD) (bottom) experimental spectra in acetonitrile for the second eluted enantiomer of **4c** on Chiralpak IG and TD-DFT calculated spectra ($\sigma = 0.39\text{ eV}$, shifted by 4 nm). Vertical bars are oscillator and rotational strengths calculated for the two conformers with arbitrary units

and TD-DFT calculations were performed on complex **3a**, and the absolute configuration deduced was identical to the one determined by X-ray diffraction (XRD).²³

The configurational stability of these palladium complexes has been studied by following the decay of enantiomeric excesses over time at 78°C in ethanol and thus enabled to determine the values of the rotational barriers (For details, see supporting information). Complex **4c** containing the benzhydryl substituent ($\Delta G^\ddagger = 117.9 \text{ kJ}\cdot\text{mol}^{-1}$; $t_{1/2} = 4.6 \text{ h}$ at 78°C) exhibited a slightly higher configurational stability than **4a** ($\Delta G^\ddagger = 111.4 \text{ kJ}\cdot\text{mol}^{-1}$; $t_{1/2} = 29 \text{ min}$ at 78°C). Of note, the rotational barrier value of **4a** was substantially lower than the calculated value ($\Delta G^\ddagger_{\text{(BB)}} = 125.5 \text{ kJ}\cdot\text{mol}^{-1}$). Compared with complex **3a** containing a dimethyl substituted unsaturated backbone ($\Delta G^\ddagger = 131.5 \text{ kJ}\cdot\text{mol}^{-1}$; $t_{1/2} = 1 \text{ h}$ at 132°C), the value of the rotational barrier of **4a** was found lower by ca. $20 \text{ kJ}\cdot\text{mol}^{-1}$, highlighting that the nature of the NHC backbone (saturated vs. unsaturated) significantly impacts its geometry and consequently the enantiomerization barriers.

3.4 | Palladium-catalyzed asymmetric intramolecular α -arylation of amides

Complexes **4a** and **4c** were tested in asymmetric catalysis for the intramolecular α -arylation of amide **13**, which represents a benchmark substrate to evaluate the efficiency of palladium complexes bearing monodentate chiral NHC ligand.^{27–30} Using the reaction conditions that have been optimized for palladium complexes **3** bearing C_1 -symmetric NHC ligands,²³ a substantial decrease in reaction yields compared with complex **3a** was observed (63%–69% vs. 91%) suggesting a lower catalytic activity of palladium complexes bearing a saturated NHC **4** (Scheme 3). However, complexes **4a** and **3a** gave oxindole **14** with identical optical purities (46%–47% ee) indicating that the nature of the NHC backbone does not

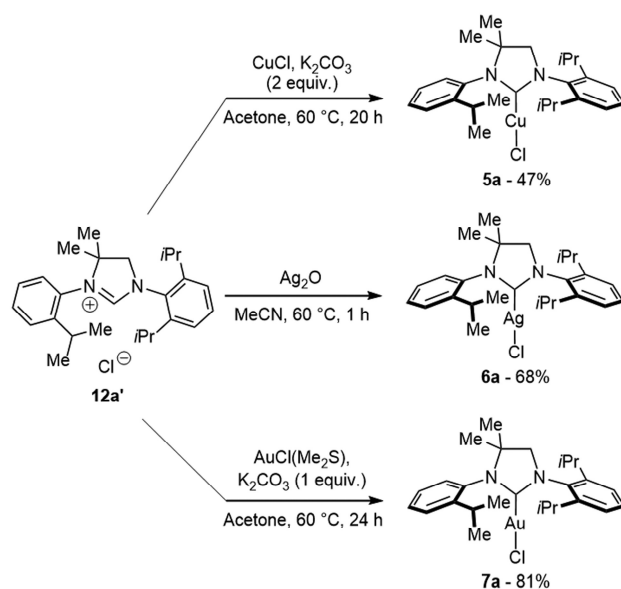


SCHEME 3 Intramolecular α -arylation of amide **13** with NHC-palladium complexes **4**

influence the ability of palladium complexes to induce enantioselectivity. The nature of the substituents decorating the *N*-aryl groups had a more pronounced effect because **4c** gave compound **14** with a significantly higher ee than **4a** (64% vs. 47%) emphasizing the favorable effect of benzhydryl compared isopropyl. Even if the efficiency of complexes **4a** and **4c** in terms of enantioselectivity could not be compared with the results that have been obtained with chiral C_2 -symmetric IKong ligands, this work highlights that configurational stabilities (values of rotational barriers) could not be correlated to the efficiency to promote a chiral induction. For example, for identical performances in asymmetric catalysis, the configurational stability of **3a** was significantly higher than the one exhibited by **4a**.

3.5 | Synthesis of other transition metal complexes, separation by chPLC and configurational stability

Then, we investigated the possibility to extend our concept of transition metal–NHC complexes containing an axial chirality to other transition metals. As depicted in Scheme 4, from imidazolium chloride **12a'**, corresponding copper complex **5a**, silver complex **6a** and gold complex **7a** were prepared in moderate to good yields following standard procedures. All of these coinage metal-based complexes were found very stable and were purified by silica gel chromatography. Of note, the stability of silver complex **6a** was remarkable because NHC–silver complexes are known for their low stability in

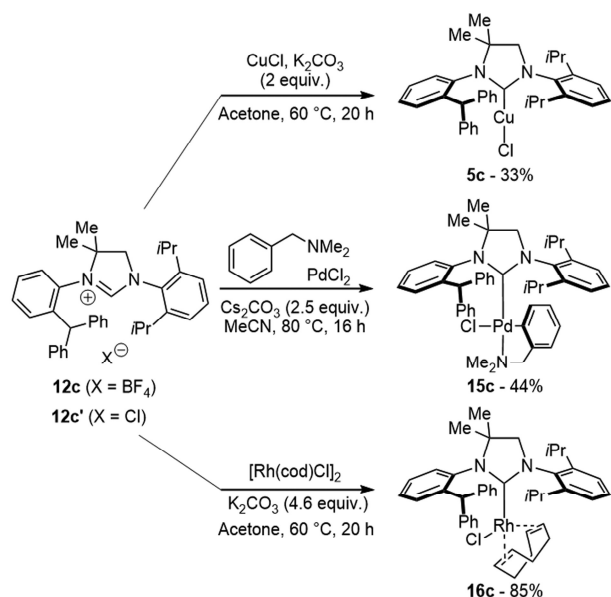


SCHEME 4 Preparation of coinage metal-based complexes

solution due to a dimerization process leading to the formation of cationic bis (NHC)Ag(I) complexes.³¹ Because these complexes did not exhibit isomeric forms, ¹H NMR spectra displayed clear signals, in particular three distinct isopropyl CH resonances. ¹³C NMR spectra of **5a** and **7a** exhibited carbenic carbon resonances at 202.1 and 194.7 ppm, respectively, which are characteristic of copper and gold complexes bearing a saturated NHC ligand. ¹³C NMR spectra of silver complex **6a** displayed two sets of doublets at 206.9 ppm corresponding to ¹⁰⁹Ag and ¹⁰⁷Ag isotopes and with different *J* coupling of 258.7 and 223.7 Hz, directly proportional to the gyromagnetic ratios of ¹⁰⁹Ag and ¹⁰⁷Ag. More surprisingly, *J*³(¹⁰⁹⁻¹⁰⁷Ag-¹³C) couplings were also observed for the backbone CH₂ carbon with resonance at 67.4 (*J*³[¹⁰⁹Ag-¹³C] = 80.9 Hz) and 67.4 ppm (*J*³[¹⁰⁷Ag-¹³C] = 65.4 Hz).

From imidazolinium chloride or tetrafluoroborate **12c**, copper-, palladacycle-, and rhodium-based complexes were prepared in low to good yields according to standard procedures for analogous complexes and purified by silica gel chromatography (Scheme 5). Like palladium complexes **4a** and **4c**, complexes **15c** and **16c** presented isomeric forms in solution. The ¹³C NMR spectrum of rhodium complex **16c** exhibited a doublet at 216.3 ppm with *J*¹(¹⁰³Rh-¹³C) = 47.9 Hz.

A thorough screening of chiral HPLC columns and eluent compositions allowed to identify suitable conditions for enantiomers separation for all complexes (For details, see supporting information). However, the low configurational stabilities of copper complexes **5a** and **5c** as well as silver complex **6a** did not permit their



SCHEME 5 Synthesis of several metal complexes from imidazolinium salt **12c**

resolution in preparative scale. Nevertheless, small quantities of enantioenriched complexes were obtained in order to determine their rotational barrier values by following the decay of enantiomeric excesses over the time at room temperature (Table 3). Enantiomers of other complexes were separated by chPLC in preparative scale, ECD spectra were recorded and their enantiomerization barriers were determined. Of note, the solvent used to perform enantiomerization experiences seemed to have a negligible influence on the enantiomerization kinetics. Thus, at 25 °C, rhodium complex **16c** has a rotational barrier of 107.2 kJ·mol⁻¹ in ethanol and 106.1 kJ·mol⁻¹ in dichloromethane (For details, see supporting information). Compared with complexes bearing unsaturated NHC ligands with two methyl substituents, complexes bearing saturated NHC ligands with a *gem* dimethyl pattern exhibited lower rotational barrier values by ca. 20 kJ·mol⁻¹ regardless the metal nature, for example, **3a** versus **4a** (131.5 vs. 111.4 kJ·mol⁻¹, Entries 1 and 2); **17a** versus **5a** (117.2 vs. 94.7 kJ·mol⁻¹, Entries 4 and 6); **17c** versus **5c** (122.0 vs. 100.7 kJ·mol⁻¹, Entries 5 and 7), or **18a** versus **7a** (142.4 vs. 122.2 kJ·mol⁻¹, Entries 9 and 10). Benzhydryl group was found slightly more sterically demanding than isopropyl as it led to increase ΔG^\ddagger by 6 kJ·mol⁻¹; **4a** versus **4c** (111.4 vs. 117.9 kJ·mol⁻¹, Entries 2 and 3) or **5a** versus **5c** (94.7 vs. 100.7 kJ·mol⁻¹, Entries 6 and 7). The values of the enantiomerization barriers seemed to be correlated to the nature of the metal, in particular their atomic radii, proving that the more favorable rotation leading to enantiomerization is taking place on the metal side as anticipated by theoretical calculations. Of note, there was a fair correlation between calculations and experiences with a ΔG^\ddagger difference of around 5 kJ·mol⁻¹, to the exception of palladium allyl complex **4a** ($\Delta\Delta G^\ddagger$ = 14 kJ·mol⁻¹). Nevertheless, the size of the metal was not the only parameter to consider because the enantiomerization barrier of silver complex **6a** would have been closer to the one of gold complex **7a** than copper complex **5a**. Because crystals suitable for XRD were obtained for these coinage metal complexes (Figure 6), allowing the confirmation of the atoms connectivity; and the determination of the absolute configuration of **7a**, bonds distances, angles, and torsion angles were scrutinized. The only noticeable difference was the length of the metal carbene bond: C_{Carbene}-Cu = 1.8845(15) Å, C_{Carbene}-Ag = 2.080(3) Å, C_{Carbene}-Au 1.982(7)/2.016(7) Å. These values are in the range of the bond distances that have been observed for similar NHC complexes.

The length C_{Carbene}-Ag bond, 10% longer than C_{Carbene}-Cu distance, explains that the enantiomerization barrier was found lower than could be expected considering only the atomic radius of silver. Bond distances from

TABLE 3 Rotational barriers values of atropisomeric NHC-TM complexes

Entry	Complex	ΔG^\ddagger (kJ·mol ⁻¹)	T (°C)	$t_{1/2}$
1	3a (Pd)	131.1	132	61 min
2	4a (Pd)	111.4	78	29 min
3	4c (Pd)	117.9	78	4.5 h
4	17a (Cu)	117.2	83	112 min
5	17c (Cu)	122.0	83	10.1 h
6	5a (Cu)	94.7	25	37 min
7	5c (Cu)	100.7	30	203 min
8	6a (Ag)	101.2	25	8.2 h
9	18a (Au)	142.4	132	26 h
10	7a (Au)	122.2	78	20 h
11	15c (Pd)	108.2	25	5.9 days
12	16c (Rh)	107.2	25	3.9 days

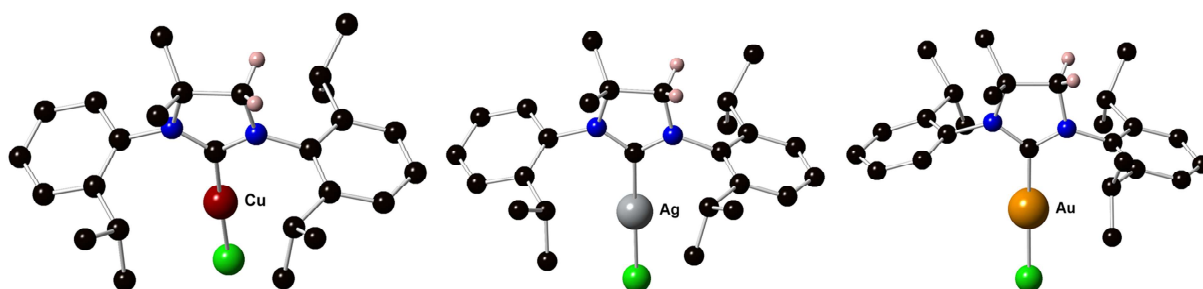
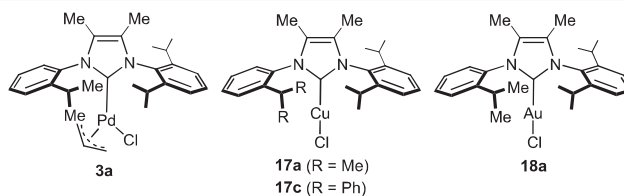


FIGURE 6 Ball-and-stick representations of complexes (*rac*)-**5a**, (*rac*)-**6a** and (*R_a*)-(-)-**7a** (most of the hydrogens have been removed for clarity)

XRD were in good agreement with the values extracted from theoretical calculations.

4 | CONCLUSION

In summary, we disclosed the synthesis of chiral transition metal complexes bearing dissymmetric NHCs containing a saturated backbone with a *gem* dimethyl moiety. These complexes were atropisomers due to the restricted rotation of the dissymmetric *N*-aryl group about the C–N bond as a result of the presence of the *gem* dimethyl pattern as well as the metal. When these complexes

presented a sufficient configurational stability, resolution by chiral HPLC in preparative scale afforded enantiomers with excellent enantiopurities (>99% ee). Enantiomerization barriers were thoroughly investigated, and it was found that a saturated backbone with a *gem* dimethyl moiety led to reduced configurational stabilities compared with unsaturated NHCs with a dimethyl substituted backbone. The nature of the transition metal, its size, and the resulting C_{Carbene}–metal bond length, played an important role on the values of the rotational barriers. However, the nature of the backbone had no influence on the enantioselectivity for the asymmetric intramolecular α -arylation of amide. The concept of atropisomeric metal–

NHC complexes and their resolution by cHPLC, which was initially developed for copper- and palladium-based complexes was extended to various other complexes, thus paving the way for future developments.

ACKNOWLEDGMENTS

We are grateful to the CNRS, Aix Marseille Université, and the ECM. M. S. thanks Aix Marseille Université for a PhD grant. We acknowledge the Agence Nationale de la Recherche (ANR-20-CE07-0030 cResolu). We thank the Spectropole (Fédération des Sciences de Marseille), in particular Dr Michel Giorgi for DRX and Dr Valérie Monnier and Mrs Gaëlle Hisler for HRMS as well as Arnaud Treuvey (ECM) for IR spectroscopy. Calculations of UV and ECD spectra were supported by the computing facilities of the CRCMM (Centre Régional de Compétences en Modélisation Moléculaire de Marseille). Umicore AG & Co is acknowledged for a generous gift of complexes.

DATA AVAILABILITY STATEMENT

Data that support the findings of this study are openly available in the supporting information of this article or are available from the corresponding author upon reasonable request.

ORCID

Muriel Albalat  <https://orcid.org/0000-0002-0215-0999>

Marion Jean  <https://orcid.org/0000-0003-0524-8825>

Nicolas Vanthuyne  <https://orcid.org/0000-0003-2598-7940>

Paola Nava  <https://orcid.org/0000-0002-8909-8002>

Stéphane Humbel  <https://orcid.org/0000-0001-5405-1848>

Damien Héroult  <https://orcid.org/0000-0001-7753-3276>

Hervé Clavier  <https://orcid.org/0000-0002-2458-3015>

REFERENCES

- Nolan SP (Ed). *N-Heterocyclic Carbenes Effective Tools for Organometallic Synthesis*. Wiley-VCH: Weinheim; 2014:568.
- Diez-González S. *N-Heterocyclic Carbenes: From Laboratory Curiosities to Efficient Synthetic Tools: Edition 2*. Cambridge, U.K.: The Royal Society of Chemistry; 2017:666.
- Huynh HV. *The Organometallic Chemistry of N-heterocyclic Carbenes*. A Textbook Series, Wiley, Hoboken: Inorganic Chemistry; 2017:368.
- Wang F, Liu L-J, Wang W, Li S, Shi M. Chiral NHC-metal-based asymmetric catalysis. *Coord Chem Rev*. 2012; 256(9-10):804-853.
- Janssen-Müller D, Schlepphorst C, Glorius F. Privileged chiral N-heterocyclic carbene ligands for asymmetric transition-metal catalysis. *Chem Soc Rev*. 2017;46(16):4845-4854.
- Czerwiński PJ, Michalak M. Synthetic approaches to chiral non-C₂-symmetric N-heterocyclic carbene precursors. *Synthesis*. 2019;51(08):1689-1714.
- Ma Y, Song C, Ma C, Sun Z, Chai Q, Andrus MB. Asymmetric addition of aryl boron reagents to enones with rhodium dicyclopentadiene imidazolium carbene catalysis. *Angew Chem Int Ed*. 2003;42(47):5871-5874.
- Check CT, Jang KP, Schwamb CB, Wong AS, Wang MH, Scheidt KA. Ferrocene-based planar chiral imidazopyridinium salts for catalysis. *Angew Chem Int Ed*. 2015;54(14):4264-4268.
- Shikata Y, Yasue R, Yoshida K. Coordination behavior of a planar chiral cyclic (amino)(ferrocenyl)carbene ligand in iridium complexes. *Chem Eur J*. 2017;23(66):16806-16812.
- Dasgupta A, Ramkumar V, Sankararaman S. Catalytic asymmetric hydrogenation using a [2.2]paracyclophane based chiral 1,2,3-triazol-5-ylidene-Pd complex under ambient conditions and 1 atmosphere of H₂. *RSC Adv*. 2015;5(28): 21558-21561.
- Iglesias-Sigüenza J, Izquierdo C, Díez E, Fernández R, Lassaletta JM. Chirality and catalysis with aromatic N-fused heterobicyclic carbenes. *Dalton Trans*. 2016;45(25): 10113-10117.
- Van Veldhuizen JJ, Garber SB, Kingsbury JS, Hoveyda AH. Recyclable chiral Ru catalyst for enantioselective olefin metathesis. Efficient catalytic asymmetric ring-opening/cross metathesis in air. *J Am Chem Soc*. 2002;124(18):4954-4955.
- Van Veldhuizen JJ, Gillingham DG, Garber SB, Kataoka O, Hoveyda AH. Chiral Ru-based complexes for asymmetric olefin metathesis: enhancement of catalyst activity through steric and electronic modifications. *J Am Chem Soc*. 2003; 125(41):12502-12508.
- Wang YM, Kuzniewski CN, Rauniyar V, Hoong C, Toste FD. Chiral (acyclic diaminocarbene)gold(I)-catalyzed dynamic kinetic asymmetric transformation of propargyl esters. *J Am Chem Soc*. 2011;133(33):12972-12975.
- Franco J, Grande-Carmona F, Faustino H, et al. Axially chiral triazoloisoquinolin-3-ylidene ligands in gold(I)-catalyzed asymmetric intermolecular (4 + 2) cycloadditions of allenamides and dienes. *J Am Chem Soc*. 2012;134(35):14322-14325.
- Handa S, Slaughter LM. Enantioselective alkynylbenzaldehyde cyclizations catalyzed by chiral gold(I) acyclic diaminocarbene complexes containing weak Au-arene interactions. *Angew Chem Int Ed*. 2012;51(12):2912-2915.
- Handa S, Lippincott DJ, Aue DH, Lipshutz BH. Asymmetric gold-catalyzed lactonizations in water at room temperature. *Angew Chem Int Ed*. 2014;53(40):10658-10662.
- Zhu S, Wang C, Zhao S, Xiao Y, Hu L, Huang Z. Modular approach to the synthesis of polydentate NHC-ligand precursors (benzimidazolium salts) containing axial chiral 1,1'-binaphthyl via Pd-catalyzed N-arylation of 1,2-diaminobenzene. *Synthesis*. 2014;46(02):212-224.
- Grande-Carmona F, Iglesias-Sigüenza J, Álvarez E, Díez E, Fernández R, Lassaletta JM. Synthesis and characterization of axially chiral imidazoisoquinolin-2-ylidene silver and gold complexes. *Organometallics*. 2015;34(20):5073-5080.
- Varela I, Faustino H, Díez E, et al. Gold(I)-catalyzed enantioselective [2 + 2 + 2] cycloadditions: an expedient entry to enantioenriched tetrahydropyran scaffolds. *ACS Catal*. 2017; 7(4):2397-2402.
- Zhang JQ, Liu Y, Wang XW, Zhang L. Synthesis of chiral bifunctional NHC ligands and survey of their utilities in asymmetric gold catalysis. *Organometallics*. 2019;38(20):3931-3938.

22. Kong L, Morvan J, Pichon D, et al. From prochiral N-heterocyclic carbenes to optically pure metal complexes: new opportunities in asymmetric catalysis. *J Am Chem Soc.* 2020; 142(1):93-98.
23. Kong L, Chou Y, Jean M, et al. C₁-Symmetric atropisomeric NHC palladium (II) complexes: synthesis, resolution and characterization. *Adv Synth Catal.* 2021;363(17):4229-4238.
24. Perrin DD, Armarego WLF. *Purification of Laboratory Chemicals*. 3rd ed. Oxford: Pergamon Press; 1988:391.
25. Fulmer GR, Miller AJM, Sherden NH, et al. NMR chemical shifts of trace impurities: common laboratory solvents, organics, and gases in deuterated solvents relevant to the organometallic chemist. *Organometallics*. 2010;29(9):2176-2179.
26. Chung CK, Grubbs RH. Olefin metathesis catalyst: stabilization effect of backbone substitutions of n-heterocyclic carbene. *Org Lett.* 2008;10(13):2693-2696.
27. Lee S, Hartwig JF. Improved catalysts for the palladium-catalyzed synthesis of oxindoles by amide α -arylation. Rate acceleration, use of aryl chloride substrates, and a new carbene ligand for asymmetric transformations. *J Organomet Chem.* 2001;66:3402-3415.
28. Kündig EP, Seidel TM, Jia YX, Bernardinelli G. Bulky chiral carbene ligands and their application in the palladium-catalyzed asymmetric intramolecular α -arylation of amides. *Angew Chem Int Ed.* 2007;46(44):8484-8487.
29. Luan X, Mariz R, Robert C, et al. Matching the chirality of monodentate n-heterocyclic carbene ligands: a case study on well-defined palladium complexes for the asymmetric α -arylation of amides. *Org Lett.* 2008;10(24):5569-5572.
30. Würtz S, Lohre C, Fröhlich R, Bergander K, Glorius F. IBiox [(–)-menthyl]: a sterically demanding chiral NHC ligand. *J Am Chem Soc.* 2009;131(24):8344-8345.
31. Su HL, Pérez LM, Lee SJ, Reibenspies JH, Bazzi HS, Bergbreiter DE. Studies of ligand exchange in N-heterocyclic carbene silver(I) complexes. *Organometallics*. 2012;31(10): 4063-4071.